Visualization of energy: light dose indicator based on electrochromic gyroid nano-materials

2015 Nanotechnology 26 225501

(http://iopscience.iop.org/0957-4484/26/22/225501)

IOP Publishing Nanotechnology
Nanotechnology 26 (2015) 225501 (6pp) doi:10.1088/0957-4484/26/22/225501

Visualization of energy: light dose indicator based on electrochromic gyroid nanomaterials

Di Wei[1,3], Maik R J Scherer[2], Michael Astley[1] and Ullrich Steiner[2]

[1] Nokia R&D UK, Broers Building, 21 JJ Thomson Avenue, Madingley Road, CB3 0FA, Cambridge, UK
[2] Cavendish Laboratory, Department of Physics, University of Cambridge, J. J. Thomson Avenue, Cambridge, CB3 0HE, UK

E-mail: di.wei@nokia.com

Received 30 January 2015, revised 9 April 2015
Accepted for publication 15 April 2015
Published 13 May 2015

Abstract

The typical applications of electrochromic devices do not make use of the charge-dependent, gradual optical response due to their slow voltage-sensitive coloration. However, in this paper we present a design for a reusable, self-powered light dose indicator consisting of a solar cell and a gyroid-structured nickel oxide (NiO) electrochromic display that measures the cumulative charge *per se*, making use of the efficient voltage-sensitive coloration of gyroid materials. To circumvent the stability issues associated with the standard aqueous electrolyte that is typically accompanied by water splitting and gas evolution, we investigate a novel nano-gyroid NiO electrochromic device based on organic solvents of 1,1,1,3,3,3-hexafluoropropan-2-ol, and room temperature ionic liquid (RTIL) triethylsulfonium bis(trifluoromethylsulfonyl) imide ([SET3][TFSI]) containing lithium bis(trifluoromethylsulfonyl) imide. We show that an effective light dose indicator can be enabled by nano-gyroid NiO with RTIL; this proves to be a reliable device since it does not involve solvent degradation or gas generation.

S Online supplementary data available from stacks.iop.org/NANO/26/225501/mmedia

Keywords: electrochromic gyroid materials, room temperature ionic liquid, visualization of electric charge, light dose indicator

(Some figures may appear in colour only in the online journal)

1. Introduction

Skin cancer is the most common type of cancer among white or Caucasian populations worldwide [1], creating demand for a self-powered, low-cost and ideally reusable light dose measuring device to monitor the accumulated exposure to sunlight or ultraviolet light. Photochromic materials that undergo a color change in a time-integrated response to light typically exhibit no or only poor/slow reversibility making their application in such sensors unfavorable [2]. In contrast, the color change of electrochromic materials caused by an electrical current is persistent, and at the same time highly reversible on current reversal. Electrochromism is generally used to control the amount of light and heat allowed to pass through 'smart windows' [3], but several attempts have been reported to facilitate this phenomena in light sensors by coupling dye sensitized solar cells with electrochromic devices.

Modifications to the classical DSSC design were made either by replacing the Pt counter electrode with an electrochromic material like tungsten trioxide (WO_3) or by adding WO_3 to the photoanode consisting of titanium dioxide nanoparticles, where Pt can accelerate the bleaching independently of the coloration [4, 5]. For these photoelectrochromic cells, coloration is attained by the photon–electron conversion without an external power source. However, the associated photovoltaic characteristics have not been demonstrated. Recently the use of a patterned electrode

[3] Author to whom any correspondence should be addressed.

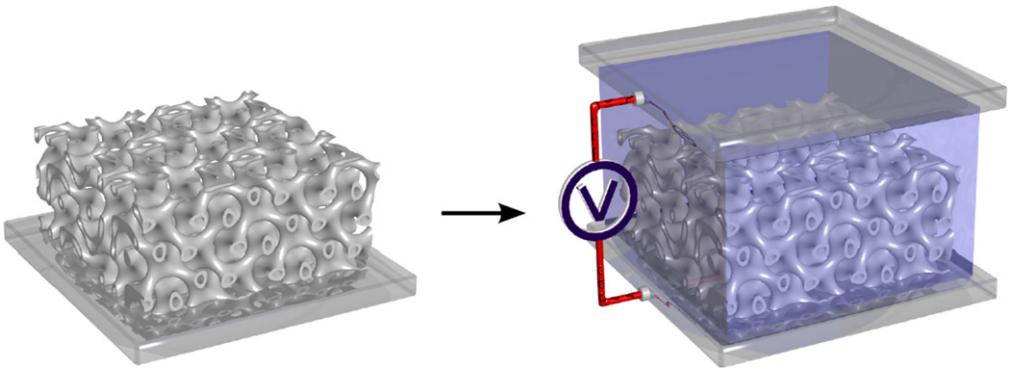

Figure 1. Schematic illustration showing the DG-structured NiO film (left) assembled into an electrochemical cell with (a) fluorine doped tin oxide glass (FTO) counter electrode (right).

containing both Pt and electrochromic WO_3 has been shown to make a fast switching photovoltachromic cell (bleaching time of 4 s) with a tuneable transmittance [6].

Electrochromism of metal oxides is based on an oxidation state change that is typically accompanied by an insertion (extraction) of ions into (from) the color changing solid causing significant volume changes [7]. The involved electrochemical redox reactions are therefore diffusion-controlled and limit the performance of bulk devices. Recent studies have shown that utilizing a gyroid structure formation on the 10 nm length scale is an effective strategy to enhance performance of electrochromic devices. The porous structure of the gyroid material helps to overcome the limitations associated with diffusion-controlled processes by increasing the active interfacial area without sacrificing its connectivity. Structuring the electrochromic material on the nanoscale was found to improve the accessibility of the ion insertion sites, reduce the ion diffusion lengths and make the material less susceptible to ageing effects caused by the repeating volume change [8, 9]. This in turn facilitated a simultaneous enhancement of the coloration contrast and response time. Efficient transport of electrons and ions through the electrochromic material and the electrolyte, respectively, requires the nanostructure itself and its mesopore network to be continuous; the 3D bicontinuous double-gyroid (DG) equilibrium structure with cubic Ia3d symmetry arising from the self-assembly of strongly segregated diblock copolymers is such a nanoscale morphology [10]. Mesoporous films prepared from these copolymers can be used for the template-assisted nanostructuring of functional materials via electrochemical replication. DG-structured electrochromic materials such as vanadium pentoxide (V_2O_5) and nickel oxide (NiO) were reported to exhibit fast switching speeds and enhanced coloration contrasts [11]. The NiO gyroid material used in this paper showed an ultra-fast electrochromic response to a change of voltage, and a bleaching time of 0.25 s was reported [9].

Due to the ultra-fast response to voltage, the voltage-dependent color changes of electrochromic materials such as V_2O_5 (blue → green → yellow) were used to visualize the charge state of a lithium ion battery [12, 13]. Furthermore, we facilitated this property to fabricate a supercapacitor based on DG-structured V_2O_5 electrodes, where the energy storage material itself indicates the charging level as a consequence of its electrochromic property [11]. Note that this intrinsic visualization of the charge state does not rely on any externally powered circuits nor does it consume any additional power. This feature is highly desirable, since it allows the continuous, power-saving indication of the charging and discharging processing of a battery or supercapacitor without the need to power on the device.

Here we present a design for a self-powered light dose measuring device consisting of a nanostructured electrochromic display connected to a solar cell. The integrated radiant flux is visualized by the gradual color change of a DG-structured NiO display utilizing its high coloration contrast which constitutes a novel way to measure the accumulated charge. The electrochromic 'memory effect' facilitates the light exposure integration over extended time periods. Additionally, we discuss a NiO gyroid electrochromic device filled with a room temperature ionic liquid (RTIL), which enables a broader electrochemical operation range and an improved coloration efficiency than comparable devices made with a traditional aqueous electrolyte.

2. Experiments

2.1. Synthesis of DG-structured nanotubular NiO electrodes

The synthesis of DG-structured nanotubular NiO electrodes for improved electrochromic displays has been reported elsewhere [9]. Briefly, polystyrene-b-poly(D,L-lactide) (MW = 21.6 kg mol^{-1}, polydispersity index = 1.09, 39.8%wt poly(lactic acid) (PLA) fraction) was spincast onto fluorine-doped tin oxide substrates (FTO) and annealed for 20 min at 173 °C to form a DG morphology. The PLA microphase was selectively degraded in an aqueous solution of pH 13 to form a network with ca. 37% porosity. The voided film was then replicated with Ni by electroplating at a constant potential of −1.05 V versus Ag/AgCl using a commercial Ni plating solution (bright finish, Alfa Aesar). Subsequently, the DG-structured Ni film was thermally oxidized at 450 °C for 10 h under an oxygen atmosphere.

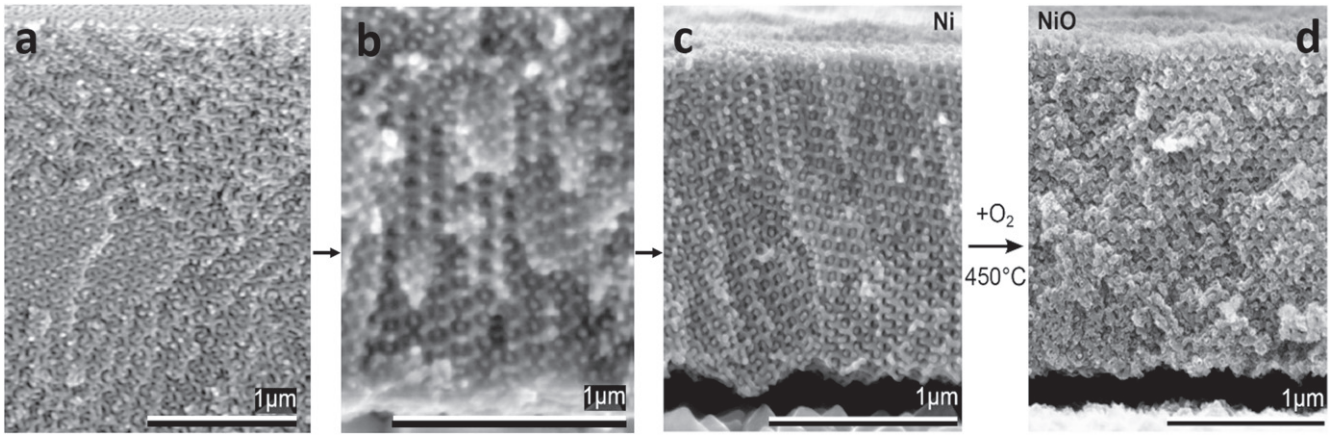

Figure 2. Cross-sectional scanning electron microscopy images of (a), self-assembled voided DG polymer films; (b), DG polymer template filled with Ni by electroplating; (c), DG-structured free standing Ni and (d), DG-structured NiO prepared on FTO. The Kirkendall effect is responsible for the transition from solid Ni struts to tubular NiO network segments [14]. Figures 2(a) and (b) were reproduced from figure 1 in [9] with permission granted from Copyright (2013) American Chemical Society.

2.2. Device assembly

Layered electrochromic cells were assembled by the following steps (figure 1): capping with a FTO counter electrode (using a pre-cut thermoplastic gasket (Parafilm) as a spacer) and fusing at 150 °C for 30 s, infiltration of the electrolyte, and finally sealing the cell with Double Bubble epoxy glue (Henkel).

The light dose sensor was made by connecting the gyroid electrochromic cell with a solar cell through a switch and passive circuit—a detailed device description is in the supplementary materials.

3. Results and discussions

DG-structured nanotubular NiO electrodes were synthesized by electroplating Ni onto a diblock-copolymer template, followed by thermal oxidization at 450 °C for 10 h under an oxygen atmosphere, as shown in figure 2. During the oxidation the solid Ni struts are transformed into nanotubular NiO network segments due to the outwards diffusion of Ni atoms from the strut core through the forming NiO shell, known as the nanoscale Kirkendall effect [14].

Transparent electrochromic devices were assembled by capping the prepared electrochromic electrodes with a FTO counter electrode using a pre-cut thermoplastic gasket as a spacer (figure 1). After infiltration of the electrolyte with a needle and syringe, the cell was sealed with epoxy glue. Before assembling the cell the NiO films were preconditioned by performing several tens of switching cycles in a 1 M KOH (aq) electrolyte (±0.55 V versus Ag/AgCl) [15].

The coloration step in an alkaline, aqueous electrolyte is typically accompanied by water splitting and gas evolution occurring at the NiO electrode. The resulting pressure increase in the sealed cell can cause bursting and leakage of the aggressive alkaline electrolyte into the environment. Therefore, the first part of this study was concerned with identifying more suitable electrolyte alternatives. Few electrochemically inert organic solvents that dissolve potassium hydroxide are known. We found that 1,1,1,3,3,3-hexafluoropropan-2-ol (HFP), which among other fluorinated alcohols is used in numerous applications in organic synthesis and as novel electrolyte for supercapacitors, dissolves KOH [16]. Furthermore, RTILs currently attract a lot of attention as 'green solvents' and superior electrolytes due to their high electrochemical stability, high boiling point and low vapor pressure [17]. Since KOH is generally insoluble in anhydrous RTILs, here triethylsulfonium bis(trifluoromethylsulfonyl) imide ([SET3][TFSI]) containing lithium bis(trifluoromethylsulfonyl) imide (LiTFSI) was studied as an electrolyte.

For comparison reasons the same ca. 550 nm thick DG structured NiO electrode (shown in figure 3(a)) was used for investigating the effect the electrolyte has on the electrochemical stability and the electrochromic performance. The electrolytes KOH in HFP, KOH in H_2O and LiTFSI in [SET3][TFSI], each with a 1 M concentration, were tested in this specific order. Between the performance tests of different electrolytes the NiO electrode was rinsed thoroughly with water, dried at 100 °C for 20 min, reassembled into a cell, and filled with the electrolyte to be investigated next. On immersion of NiO into an alkaline solution a spontaneous chemical conversion into a hydrous metal oxide phase Ni $(OH)_2$ takes place [15]. The Ni(II)/Ni(III) couple responsible for the reversible color change on electrochemical cycling in an alkaline aqueous electrolyte has been identified as the nickel hydroxide/oxy-hydroxide phases [15, 18]

$$Ni(OH)_2 \rightleftharpoons NiOOH + H^+ + e^-.$$

In contrast, the color change in an anhydrous electrolytes containing lithium salt may be caused by the insertion (extraction) of Li^+ cations into (from) the NiO or the nickel hydroxide/oxy-hydroxide matrix [19, 20].

Transmittance spectra of the bleached and colored state of the electrochromic device filled with the different electrolytes are shown in figure 3(b). The applied switching

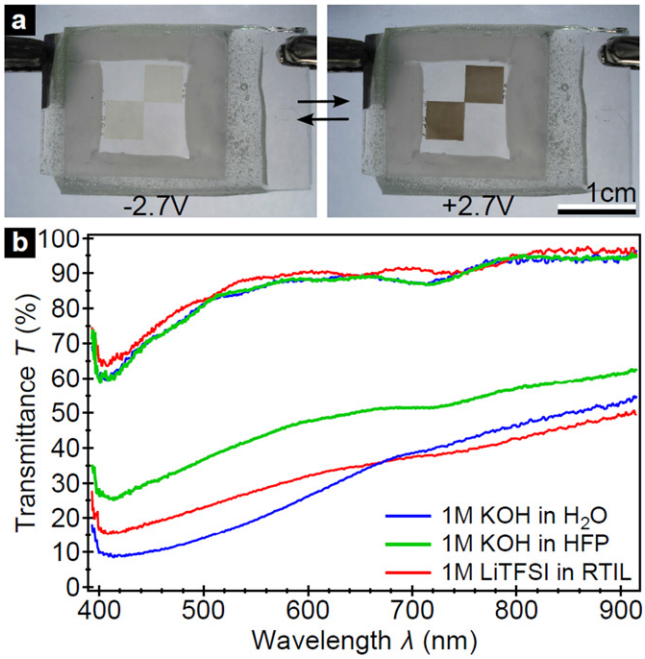

Figure 3. (a) Photographs of the electrochromic display filled with RTIL in the bleached (colored) state before (after) illumination of the solar cell; (b), transmittance spectra of the electrochromic devices for the three electrolytes tested.

Table 1. Electrochromic performance at $\lambda = 550$ nm of the same NiO electrode tested with different electrolytes.

	V (V)	ΔT (%)	CE ($cm^2\,C^{-1}$)
HFP	-2.0 ± 2.0	43	−95
Water	-1.6 ± 2.0	66	−82
RTIL	-2.7 ± 2.7	61	−104

potentials V and the optical coloration contrast $\Delta T = T_b - T_c$ at a wavelength of $\lambda = 550$ nm, as defined by the fully bleached (T_b) and colored (T_c) state, are summarized in table 1. The highest contrast was observed in the case of the aqueous solution which significantly outperforms the HFP electrolyte [15]. The Li^+-containing RTIL system also exhibits a similar high coloration contrast.

In order to determine appropriate switching potentials the optical behavior at $\lambda = 550$ nm during cyclic voltammetry (CV) was recorded (figures 4(a) and S1(a)). In all three systems a steep change in transmittance occurs at the redox peak potentials giving rise to hysteresis. In case of HFP and water the sharp increase in current at potentials exceeding +2 V is due to solvent degradation/water splitting and is accompanied by gas evolution. With an inferior coloration contrast and similar electrochemical stability, the use of HFP as an electrolyte solvent does not present any advantages over water. The current increase for potentials above +3 V indicates a reaction of the RTIL electrolyte; however, no gas evolution was observed (figure 4(a)).

Application of the electrochromic NiO in a calibrated light dose indicator requires knowledge of the optical density $\Delta OD = \ln(T/T_0)$ dependence on the accumulative charge density Q, where T_0 is the initial transmittance. All three systems show an approximately linear correlation between ΔOD and Q, giving rise to a fairly constant composite coloration efficiency $CE = \Delta OD/Q$ (figures 4(b) and S1(b)) [7, 19, 21]. The CE was measured by applying an alternating step potential V and integrating the corresponding current density, as summarized in table 1. The CE value for the aqueous electrolyte presented here is more accurate than that previously reported ($-47\,cm^2\,C^{-1}$), determined through slow CV measurements which suffer from a higher charge loss [9]. The excellent CE values of the RTIL-based device stem from the superior electrochemical stability resulting in less charge being lost to side reactions, i.e. electrolyte degradation and water splitting.

Impedance spectroscopy was used to study the chemical species and processes involved in the redox reactions. The dynamic behavior of ion insertion and extraction in electrochromic NiO is determined by mass transport/diffusion [22]. A linear relationship at low frequencies in the ac impedance data corresponds to a linear diffusion process of the oxidized and reduced species (known as the 'Warburg' impedance); the slope contains information about the type of diffusion [23, 24]. In the case of the aqueous electrolyte, the impedance slopes shown in figure 4(c) are steeper for negative voltages (−1 and −2 V) than for positive voltages (+1 and +2 V), indicating a more capacitive response and the insertion of cations into the electrochromic material during cathodic bleaching. This observation is consistent with the sharp peak present in the cyclic voltammogram at around −1 V (figure 3(a)), and therefore may be attributed to the insertion of potassium cations into the NiO electrode. In combination with the RTIL electrolyte the electrochromic device shows similar impedance slopes for +1, +2 and −1 V, whereas for −2 V a steeper slope is observed (figure 4(c)). This data suggests Li^+ cation insertion into the NiO at about −2 V which coincides with the sharp peak of the cathodic CV scan (figure 4(a)).

This DG-structured NiO display can be applied in a reusable, self-powered light dose indicator. The sensor design (figure 5(a) and figure S_2) consists of three building blocks: (1) a photovoltaic cell that acts as combined power source and as light-sensitive element; (2) a passive electric circuit that adjusts the solar cell's potential/current and resets the sensor; and (3) an electrochromic display for the simultaneous measurement and visualization of the light dose. More specifically, a Nokia silicon solar panel and the resistor values specified in figure 5(a) were used. A NiO device filled with the RTIL electrolyte was chosen since it outperformed the HFP and aqueous system in terms of electrochemical stability and safety aspects while exhibiting similar/superior electrochromic properties.

In sensing mode, with S_1 switched as shown in figure 5(a), the resistor R_3 is disconnected and the load resistance connected to the photovoltaic panel is $R_L \approx R_1$, since $R_1 \ll R_2$. The solar cell output voltage and current are defined by the intersection of the linear J/V curve of the load resistor R_L with the light intensity-dependent J/V curve of the solar cell (see supplementary data and figure S3). The voltage

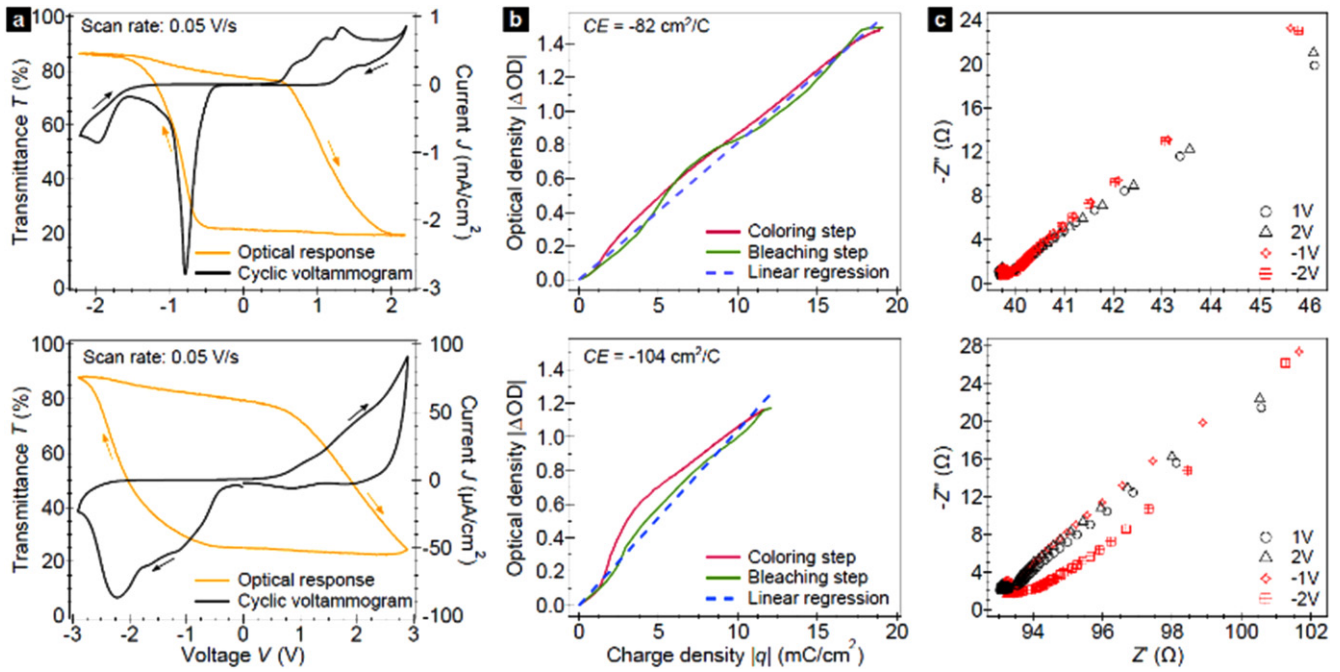

Figure 4. Electrochemical and optical characterization of the NiO electrochromic devices with an aqueous (top) and RTIL electrolyte (bottom). (a) Cyclic voltammogram and corresponding optical response at $\lambda = 550$ nm. Scan rate: 50 mV s^{-1}; (b), relation between the charge density and the optical density at $\lambda = 550$ nm—the slope defines the coloration efficiency CE; (c), impedance spectroscopy data measured with an amplitude of 10 mV in the frequency range from 1 MHz to 0.1 Hz.

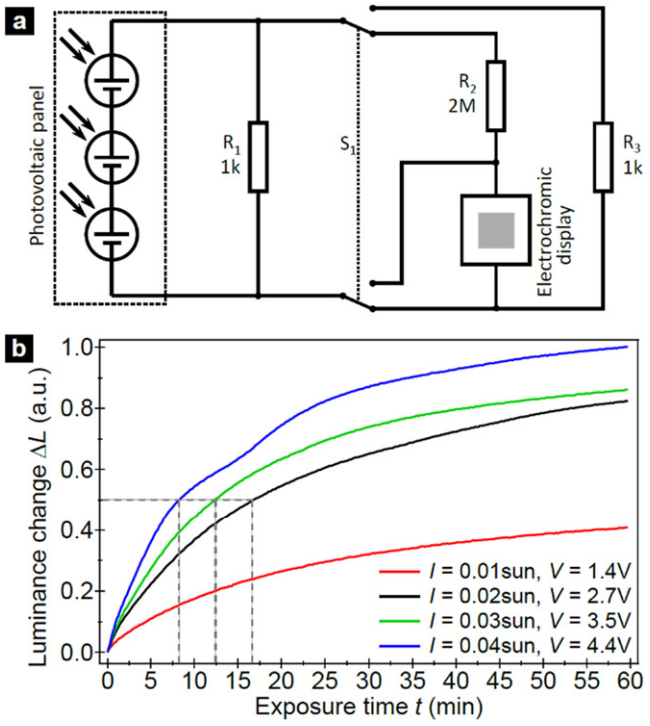

Figure 5. (a) Circuit diagram of the light dose indicator with the switch S_1 in the sensing mode position. The electrochromic display functions as combined measuring and visualization element. (b) Time-dependent luminance change ΔL of the electrochromic display for different light intensities I. Below $\Delta L \approx 0.5$ the sensing time necessary to reach a particular luminance change is inversely proportional to the light intensity. The solar panel output voltage V is given in the legend.

applied across the electrochromic device is controlled by R_2 which is connected in series. The parallel circuit with $R_1 \ll R_2$ limits the current through the NiO device to a few microamps, enabling the sensor to measure the light dose over a long period of time. When actuating switch S_1, the current is reversed and the series resistor R_2 is replaced by $R_3 \ll R_2$ to quickly reset the electrochromic device.

The light dose indicator was tested under four constant light intensity ($I = 0.01$, 0.02, 0.03 and 0.04 sun) conditions over a sensing period of 60 min. The time-resolved luminance change ΔL of the electrochromic cell was extracted from transmission micrographs (figure S4) and is displayed in figure 5(b). The solar cell output voltage $V = 1.4$ V generated at $I = 0.01$ sun lies below the sensing threshold and a complete color change is not reached within 60 min. In contrast, under brighter light conditions (0.02, 0.03 and 0.04 sun) the charge-dependent electrochromic response (see figure 5(b)) leads to a calibrated visualization of the light dose. Below $\Delta L \approx 0.5$ the sensing time necessary to reach a particular luminance change is, in first approximation, inversely proportional to the light intensity (figure 5(b)). On further light exposure, the luminance change slows due to the fact that the NiO display itself builds up a counter potential which increases together with the involved electrochemical redox process. Calibration of the sensor for higher light intensities and extended sensing periods is easily facilitated by adjusting the resistor values.

It should also be noticed that the electrochromic NiO gyroid material used in the light dose sensor is very stable. SEM images (figure S5) of such an electrode after 1000 switching cycles confirmed its morphology showed no distinguishable structural changes from the as-made one.

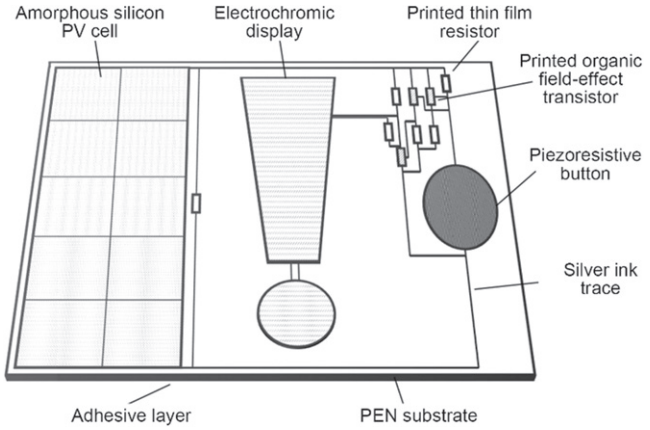

Figure 6. Design for a light dose indicating sticker for sunbathing.

A possible design of a fully flexible electrochromic light dose indicator sticker can be made as shown in figure 6. The proposed device is fabricated onto a thin plastic sheet, such as polyethylene naphthalate, consisting of the following flexible components: an amorphous silicon solar cell, an electrochromic display made from DG structured material filled with a gel electrolyte, and printed electronic components including resistors (thin metal or carbon films), conducting paths (silver ink), and a reset switch (piezo-resistive material). Fabricated as a low-cost sticker and attached to a sun lotion tube it could be used to conveniently monitor exposure during sunbathing, indicating when a critical exposure limit has been reached, thereby reducing the risk of skin cancer. The design could be further optimized for sunbathers by placing a filter that only transmits UVA/UVB on top of the solar panel. Adjusting the resistor values would facilitate taking a certain sun protection factor into account.

4. Conclusions

In summary, the application of a lithium salt containing RTIL as electrolyte was demonstrated to improve the electrochemical stability and the coloration efficiency of a DG structured NiO electrochromic display. This device was successfully applied as a combined measuring and visualization element in a light dose indicator. The presented simple sensor design is only based on a passive electronic circuit that makes an external power source unnecessary and enables miniaturization. The proposed design for a low-cost, reliable, reusable and fully flexible light dose indicator would allow production for the mass-market and could help to reduce skin cancer risk during sunbathing.

Acknowledgments

This work was funded through the Nokia–Cambridge University Strategic Research Alliance in Nanotechnology.

References

[1] Worldwide Cancer Statistics 2014 *World Cancer Research Fund International* (www.wcrf.org/)
[2] Innovative Sensors and Indicators 2014 *Insignia Technologies* (www.insigniatechnologies.com)
[3] Niklasson G A and Granqvist C G 2007 *J. Mater. Chem.* **17** 127–56
[4] Bechinger C, Ferrere S, Zaban A, Sprague J and Gregg B 1996 *Nature* **383** 608
[5] Hauch A, Georg A, Baumgartner S, Opara Krasovec U and Orel B 2001 *Electrochim. Acta* **46** 2131
[6] Wu J, Hsieh M, Liao W, Wu W and Chen J 2009 *ACS Nano* **3** 2297
[7] Granqvist C G 1995 *Handbook of Inorganic Electrochromic Materials* (Amsterdam: Elsevier)
[8] Scherer M, Li L, Cunha P, Scherman O and Steiner U 2012 *Adv. Mater.* **24** 1217–21
[9] Scherer M and Steiner U 2013 *Nano Lett.* **13** 3005–10
[10] Crossland E J W, Nedelcu M, Ducati C, Ludwigs S, Hillmyer M A, Steiner U and Snaith H J 2009 *Nano Lett.* **9** 2813–9
[11] Wei D, Scherer M, Bower C, Andrew P, Ryhanen T and Steiner U 2012 *Nano Lett.* **12** 1857
[12] Wei D, Radivojevic Z, Bower C, Andrew P and Ryhanen T 2009 Battery Cell *Patent Specification* US12611389
[13] Wei D, Radivojevic Z, Bower C, Andrew P and Ryhanen T 2011 Battery Cell With Charge State Viewable By User *Patent Specification* WO/2011/055300
[14] Yin Y, Rioux R M, Erdonmez C K, Hughes S, Somorjai G A and Alivisatos A P 2004 *Science* **304** 711–4
[15] Bouessay I, Rougier A, Poizot P, Moscovici J, Michalowicz A and Tarascon J M 2005 *Electrochim. Acta* **50** 3737–45
[16] Francke R, Cericola D, Kotz R, Weingarth D and Waldvogel S R 2012 *Electrochim. Acta* **62** 372
[17] Armand M, Endres F, MacFarlane D R, Ohno H and Scrosati B 2009 *Nat. Mater.* **8** 621–9
[18] Liu H, Yan G, Liu F, Zhong Y and Feng B 2009 *J. Alloys Compd.* **481** 385–9
[19] Campet G *et al* 1991 *Mater. Sci. Eng.* B **8** 303–8
[20] Decker F, Passerini S, Pileggi R and Scrosati B 1992 *Electrochim. Acta* **37** 1033–8
[21] Monk P, Mortimer R and Rosseinsky D 2007 *Electrochromism and Electrochromic Devices* (Cambridge: Cambridge University Press)
[22] Bohnke C and Bohnke O 1990 *Solid State Ion.* **39** 195
[23] Bisquert J, Garcia-Belmonte G, Fabregat-Santiago F and Bueno P R 1999 *J. Electroanal. Chem.* **475** 152–63
[24] Brett C M A and Brett A M O 1993 *Electrochemistry* (Oxford: Oxford University Press) p 224